
Three-Dimensional Clinical PET in Lung Cancer: Validation and Practical Strategies

Raquel Calvo, Josep M. Martí-Climent, José A. Richter, Ivan Peñuelas, Aurora Crespo-Jara, Luis M. Villar, and María J. García-Velloso

Department of Nuclear Medicine, Navarra University Hospital, Pamplona, Spain

The feasibility of 3-dimensional acquisition mode for semiquantitative analysis in thoracic PET studies was compared to the conventional 2-dimensional mode. Several practical considerations were analyzed to propose an optimized scanning protocol for clinical use. **Methods:** Twenty-one patients with focal thoracic abnormalities were evaluated with FDG PET. The acquisition consisted of 3 consecutive static scans for a single bed position: 3-dimensional (10 min), 2-dimensional (15 min), and 3-dimensional (5 min). On the basis of the average and maximum activity values per region of interest, standardized uptake value (SUV) normalized for total body weight (TBW), lean body mass (LBM), body surface area (BSA), and blood glucose level (PGL) were evaluated. The effect of the delay between tracer injection and PET scanning on the SUV, as well as on the relative error of the activity distribution, was studied from 40–134 min after tracer injection. **Results:** A strong positive correlation was observed among SUVs from 2-dimensional and both 3-dimensional acquisitions. The mean SUV percentage differences between both acquisition modes were about 17%, differences that were not statistically significant when time postinjection was addressed in the analysis of covariance. SUVs provided the greatest variability and differences among studies on experimental periods up to 70 min postinjection. Indeed, the variability of 20% observed on the SUVs from 2 PET scans 13 min apart was reduced to 9% when the acquisitions started at least 70 min after tracer injection. In addition, a two-fold reduction in the relative error of the activity distribution was observed over this period of time. The reproducibility coefficient was increased from 0.87 to 0.95 before and after 70 min postinjection, respectively. No correlation was found between different normalization procedures of SUV and LBM, BSA, TBW, or height, whereas a weak correlation was found between SUV and PGL. **Conclusion:** ^{18}F -FDG 3-dimensional PET is a realistic alternative to the gold standard 2-dimensional for clinical nonkinetic studies. A short, 5-min 3-dimensional acquisition at 70 min postinjection is proposed as the best protocol for the clinical evaluation of thoracic pathologies.

Key Words: three-dimensional PET; lung cancer; FDG; SUV

J Nucl Med 2000; 41:439–448

The ability to directly measure and correct the attenuation of annihilation photons makes PET an inherently quantitative

procedure to accurately measure physiological processes *in vivo*.

Since 1990, an increased number of commercial scanners with retractable septa have been installed in PET centers worldwide. Compared with the 2-dimensional approach, 3-dimensional PET data acquisition offers the advantage of a 5- to 7-fold increased sensitivity (1). This may be particularly beneficial when there is a need to limit the injected dose, as in scanning children and in ^{15}O -water activation studies, to reduce the imaging time, or to improve image statistics as in low-counting-rate ligand studies. To a large extent, these procedures are qualitative, but work is still continuing on quantitative studies.

Once the septa are removed, the effects of scatter, random, and dead time can no longer be ignored, if quantitative measurements are required. Thus, if 3-dimensional PET must be considered as quantitative as 2-dimensional PET, accurate corrections for attenuation and scatter are needed. Using a variety of scatter approaches, several authors have reported that 3-dimensional PET with scatter and attenuation correction is as accurate as 2-dimensional PET in phantom studies (2–3) and neuroimaging (4–5), although only preliminary results have been published for abdominal (6) and cardiac (7) PET studies. However, despite the increasing number of PET scanners capable of performing 3-dimensional imaging of the torso, many of the issues involved in the daily clinical practice have not yet been studied. One purpose of this study is to investigate the feasibility of 3-dimensional nonkinetic quantitative analysis in patients with nodular lung lesions.

Thoracic tumors represent a particular challenge for oncologists, because these tumors are not always readily accessible for tissue diagnosis without invasive procedures. PET imaging with FDG has been shown to be useful in the clinical management of lung cancer patients at various stages of the disease, including differential diagnosis of solitary nodules, initial preoperative staging of the nodal extent of non-small cell lung cancer, detection of unsuspected metastases, and differentiation or demonstration of suspected recurrence (8–18). Table 1 summarizes the main reported studies including details of the acquisition protocols and analysis techniques.

The majority of the studies just mentioned, as well as most FDG PET tumor studies in which a differential

Received Jan. 4, 1999; revision accepted Jun. 21, 1999.

For correspondence or reprints contact: José A. Richter, MD, Navarra University Hospital, Department of Nuclear Medicine, Pio XII s/n, Pamplona 31080, Spain.

diagnosis was sought, have been based on nonkinetic evaluation of tumor FDG uptake compared with injected dose per body weight (19–20). Such semiquantitative analysis, commonly referred to as standardized uptake value (SUV) or differential uptake rate (DUR), has been widely used as a compromise between the cumbersome kinetic method and simple visual assessment (21–23). However, SUV is dependent on many individual patient characteristics, including blood glucose level (PGL), total body weight (TBW), lean body mass (LBM), and body surface area (BSA). In an attempt to further classify this dependency, other studies have been reported (24–28). In addition, some other intrinsic and methodological considerations must be controlled, such as the effect of tissue heterogeneity, region size, partial volume effect, and the time elapsed between tracer injection and PET scanning (uptake period).

In an effort to establish an optimized scanning protocol and assess the impact of 3-dimensional acquisition mode in thoracic studies, our aims were to determine whether the 3-dimensional mode was a valid alternative to the conventional 2-dimensional nonkinetic analysis in patient studies and to compare the quantitative accuracy of different normalization procedures for the uptake values obtained in both acquisition modes.

MATERIALS AND METHODS

Patients

Twenty-one patients (17 men, 4 women) were referred to our institution for evaluation by FDG PET imaging. The patients were divided into 3 groups: 10 patients with undetermined lung masses, 6 with suspected recurrence of previously proven treated lung carcinoma, and 5 with proven nonlung malignancy and a chest

mass suggesting metastatic disease. A summary of the patients' characteristics is given in Table 2.

Histopathological data were obtained by mediastinoscopy and biopsy. At the time of the PET studies, none of the patients had undergone radiotherapy or chemotherapy. Patients fasted for at least 4 h before PET imaging. Serum glucose level was measured with blood glucose reagent strips and photometric measurement. Mean glucose levels were 93.05 ± 11.99 (range, 72–118). None of the patients were known to have diabetes. All patients were enrolled in the study after they were properly informed and gave consent to participate. The Ethics Committee of the Navarra University Hospital, Pamplona, Spain, approved the experimental protocols.

PET Imaging

Subjects were studied using both 2-dimensional and 3-dimensional data acquisition with a whole-body scanner ECAT EXACT HR⁺ (Siemens/CTI, Knoxville, TN) with a maximum field of view (FOV) of 15.5 cm in axial direction, allowing the imaging of 63 transaxial slices simultaneously. The scanner is equipped with retractable tungsten septa, allowing operation in both 2-dimensional and 3-dimensional modes. The lower and upper energy discriminator levels were 350 and 650 keV, respectively. Technical specifications for this scanner and its performance may be found elsewhere (29).

Seven-minute transmission scans (yielding approximately 50 million counts per bed position) were acquired before the administration of FDG and used for attenuation correction of emission data.

The protocol was started after intravenous injection of 431 ± 91 MBq (range, 343–679 MBq) FDG, properly centering the suspected pulmonary lesions on the middle of the FOV. Acquisition consisted of 3 consecutive static scans for a single bed position according to the following protocol: 10-min 3-dimensional scan (study₁), 15-min 2-dimensional scan (study₂), and 5-min 3-dimensional scan

TABLE 1
Acquisition Protocols of FDG PET Studies in Lung Cancer

Authors	Year	PET scanner/ acquisition mode	Imaging time	Time postinjection	Analysis
FDG PET in solitary pulmonary nodules					
Kubota et al.	1990	PT 931/04/2D	9 frames/5 min	30–40 min	TMR
Gupta et al.	1992	ECAT/2D	Not reported	60 min	SUR
Patz et al.	1993	GE 4096 Plus/2D	1 static 20 min	30 min	SUR
Lowe et al.	1994	GE 4096 Plus/2D	1 static 20 min	30 min	SUR
Hübner et al.	1996	ECAT 931-08-12/2D	Dynamic 1 static 15 min	0–50 min 50 min	Patlack SUV
Staging of lung cancer					
Regé et al.	1993	PT 931/08/2D	Not reported	30 min	Visual
Wahl et al.	1994	ECAT 931/2D	Dynamic 1 static 10 min	0–60 min 60 min	Visual SUVlean
Duhaylongsod et al.	1995	GE 4096 Plus/2D	20 min	30–60 min	SUR
Bury et al.	1996	Penn PET/3D	10 beds/4–8 min bed	Not reported	Visual
Steinert et al.	1997	GE 4096 Plus/2D	6 beds/6 min bed	40 min	Visual
Higashi et al.	1997	Headtom IV/2D	10–20 min	40 min	TMR

2D = 2-dimensional; 3D = 3-dimensional; TMR = tumor–muscle ratio; DUR = differential uptake ratio; SUV = standard uptake value; SUVlean = SUV corrected by lean body mass; SUR = standard uptake ratio; Patlack = Palack graphical analysis.

PT 931/04 is manufactured by CTI, Knoxville, TN; ECAT, by Siemens/CTI, Knoxville, TN; GE 4096 Plus, by General Electric Medical Systems, Milwaukee, WI; Penn PET, by UGM Medical Systems, Philadelphia, PA; and Headtom IV, by Shimazu, Kyoto, Japan.

TABLE 2
Patient Characteristics

Patient no.	Age (y)	Sex	Histopathology	Dose (MBq)	PGL (mg/100 ml)	Weight (kg)	LBM (kg)	BSA (m ²)
1	71	M	Small cell ca	471	85	84	68	1.96
2	60	M	Squamous cell	472	110	75	66	1.86
3	50	F	Ductal ca	356	93	55	44	1.49
4	64	M	Mixed ca	417	89	81	63	1.89
5	74	M	Adeno ca	344	90	73	64	1.81
6	77	M	Adeno ca	347	101	73	59	1.78
7	63	M	Adeno ca	442	81	83	69	1.96
8	72	M	Undifferentiated	395	90	77	55	1.80
9	42	M	Adeno ca	441	88	80	75	1.97
10	52	F	Adeno ca	388	80	76	56	1.82
11	44	M	Squamous cell	662	108	107	81	2.29
12	54	M	Squamous cell	455	92	69	61	1.75
13	52	M	Adeno ca (colon)	679	118	92	78	2.12
14	75	M	Squamous cell	391	107	72	61	1.78
15	51	M	Non-small cell ca	405	82	75	66	1.86
16	56	F	Adeno ca	348	95	81	45	1.77
17	64	M	Adeno ca	384	95	78	63	1.87
18	52	M	Adeno ca	399	72	76	78	1.95
19	23	F	Adeno ca	343	87	52	48	1.49
20	69	M	Squamous cell	498	81	79	66	1.90
21	51	M	Squamous cell	423	110	77	63	1.85

PGL = plasma glucose levels at time of injection; Small cell ca = small cell carcinoma; Squamous cell = squamous cell carcinoma; Ductal ca = ductal carcinoma; Mixed ca = mixed carcinoma; Adeno ca = adenocarcinoma.

(study₃). Acquisitions were started 59.81 ± 16.36 (range, 40–105), 73.71 ± 15.84 (range, 51–115), and 92.05 ± 16.33 (range, 70–134) min after FDG injection. About 3.2×10^8 , 3.7×10^6 , and 1.2×10^8 total counts for the entire datasets were collected, respectively.

Data Processing

Emission scans were reconstructed by two- and three-dimensional filtered backprojection algorithms using a Hanning filter with a cutoff frequency of 0.4, resulting in a transverse spatial resolution of 7.3×7.5 mm full width at half maximum 2-dimensional (7.7×7.7 3-dimensional). Sinograms were corrected for dead time losses, random events, arc correction, attenuation, activity decay, and scanner normalization.

Two regions of interest (ROIs) consisting of 3×4 and 1 pixel, were placed carefully on the plane of highest activity concentration for each tumor lesion. A semiautomated algorithm that searches the most intense mean count per pixel was used to place the ROI.

The mean \pm SD of the SUVs was obtained for the 3 acquisitions modes on the 2 regions, and the possibility of replacing conventional 2-dimensional with 3-dimensional acquisition mode was evaluated by a statistical correlation of both acquisitions.

The intrasubject variability of SUVs depending on the acquisition mode was quantified by the mean percentage difference with the following formula:

$$\frac{100}{n} \sum_{i=1}^n \frac{|X_{ik} - X_{ij}|}{\bar{X}_i}$$

where j and k are the 2 acquisitions compared, n is the total number of foci studied, X_{ik} (X_{ij}) are the SUV of the i focus in the k(j) study, and \bar{X}_i is the mean SUV of the X_{ik} and X_{ij} (i.e., $[X_{ik} + X_{ij}]/2$). The

mean and SD were evaluated for all foci. To evaluate the significance of the difference between studies taking into account the distortion introduced by the time between tracer injection and PET scanning, analysis of variance with time as covariant (ANCOVA) was calculated. Linear regression was performed to assess the dependency of SUVs on time after injection. The requirement of normal distribution with same variance for the linear regression analysis was achieved by the logarithmic transformation (30). The reproducibility of SUVs over time was performed by the calculation of the reliability coefficient, because the results of two-dimensional and three-dimensional data from the same subject were considered here as repeated measurements. The reliability coefficient measures intraclass correlation, i.e., the correlation between 2 measurements observed in the same individual at different times (31,32). A 1-way ANOVA using foci as independent variables was calculated for determination of the intraclass correlation coefficient. The correlation coefficient was obtained from the F statistics of the ANOVA as follows: $r = (F - 1)/(F + n - 1)$, where n is the number of measurements for each subject. The relative error of $SUV_{[avg]}$, calculated as 100 times the spatial coefficient of variation of frame counts over the 12-pixel ROI ($100 \times SD/mean$ on $SUV_{[avg]}$), was studied to estimate combined effect of tumor's intrinsic heterogeneity and ROI count statistics.

FDG uptake values in each focus was normalized to the injected dose and the patient's TBW, LBM, BSA, and PGL, all of which were calculated using previously published formulas (25,28). Linear regression analysis was performed for statistical correlation of the different normalized uptake values and the parameters referred to previously. Because SUV_{BSA} has units of m² and the rest of the normalization renders dimensionless parameters, a normaliza-

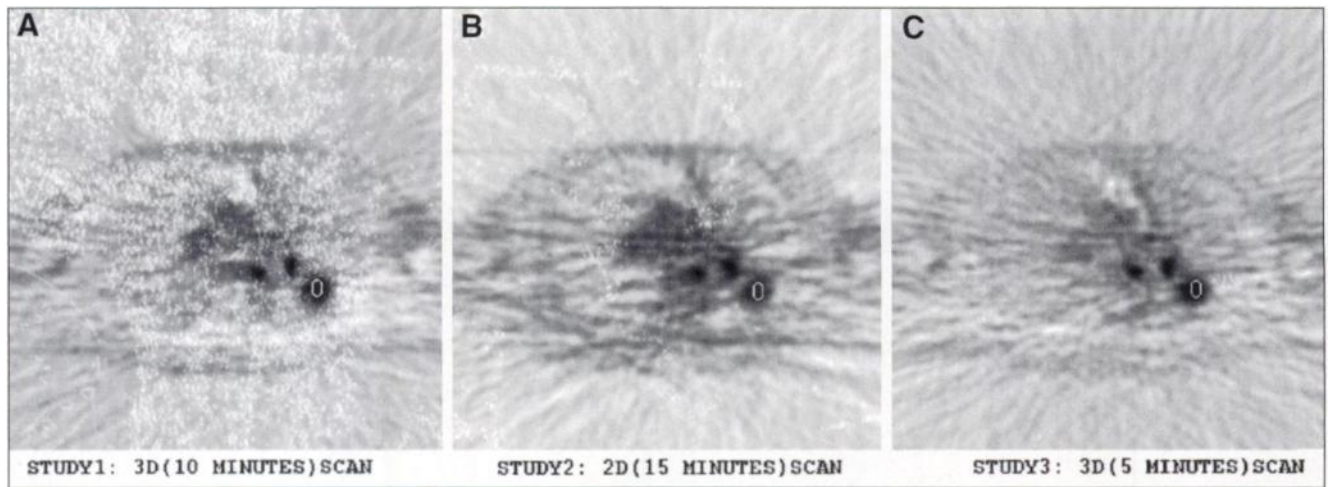


FIGURE 1. Transaxial images of patient with left lobe primary adenocarcinoma (patient 5). Three scans were obtained consecutively at 48 (A), 58 (B), and 76 (C) min postinjection and attenuation corrected. A 3×4 pixel ROI is shown.

tion with SUV (the most commonly performed) was achieved by dividing each of SUV_{BSA} values by the mean SUV_{BSA} and multiplying by the mean SUV (25).

RESULTS

A total number of 53 foci were found in 21 patients. Figure 1 shows a representative example of sequential thoracic FDG PET scans and selected ROIs obtained in patient 5.

The SUVs of the foci distribution obtained from averaged activity within each ROI ($SUV_{[avg]}$) and maximum activity ($SUV_{[max]}$), from study₁ (10 min, 3-dimensional scan), study₂ (15 min, 2-dimensional scan), and study₃ (5 min, 3-dimensional scan) are shown in Figure 2. A strong correlation among data from 2-dimensional and those derived from the 2 3-dimensional acquisitions was obtained from the 2 ROI sets (Fig. 3).

ANCOVA with foci and acquisition mode (study₁, study₂,

and study₃) as a main effect and time as covariant was calculated. Results of this analysis showed no significant difference in the two-dimensional and three-dimensional comparison between the $SUV_{[avg]}$ values, although a borderline nonsignificant difference was found when the $SUV_{[max]}$ values were used ($P = 0.293$ and $P = 0.057$, respectively). In addition, $SUV_{[avg]}$ values showed higher reproducibility than $SUV_{[max]}$ values, as indicated by their reliability coefficients (0.90 and 0.85, respectively).

In Table 3, linear regression analysis between SUVs and the acquisition start time are shown for the 3 studies. Results showed that values from study₃ (time postinjection between 70 and 134 min) produced a less steep slope, lower r values, and higher P values than those from study₁ or study₂ (in which the time postinjection ranged from 40–105 min and 51–115 min, respectively), indicating that SUVs were less dependent on time as the time postinjection increased.

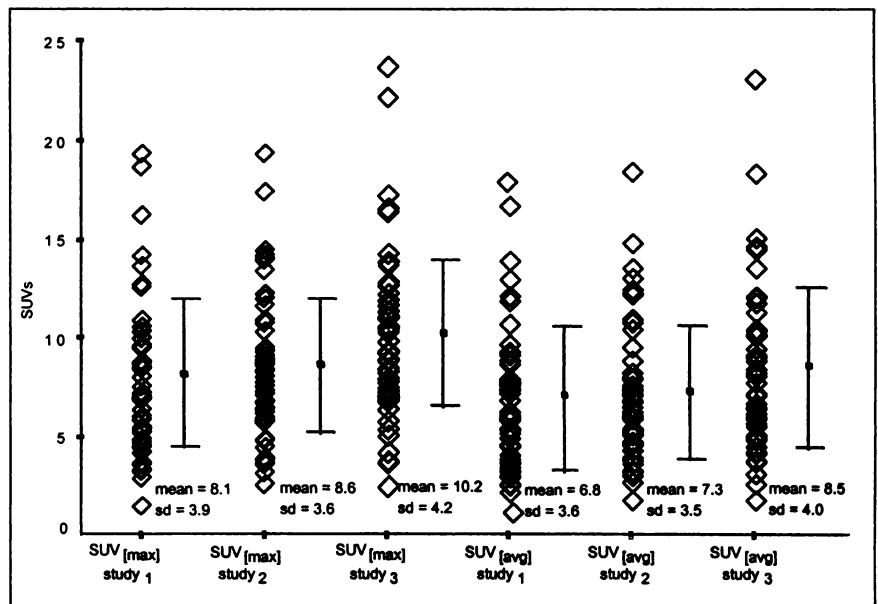


FIGURE 2. Distribution of standard uptake values, both for average and maximum region value, on study₁, study₂, and study₃. Mean \pm SD is shown for each dataset.

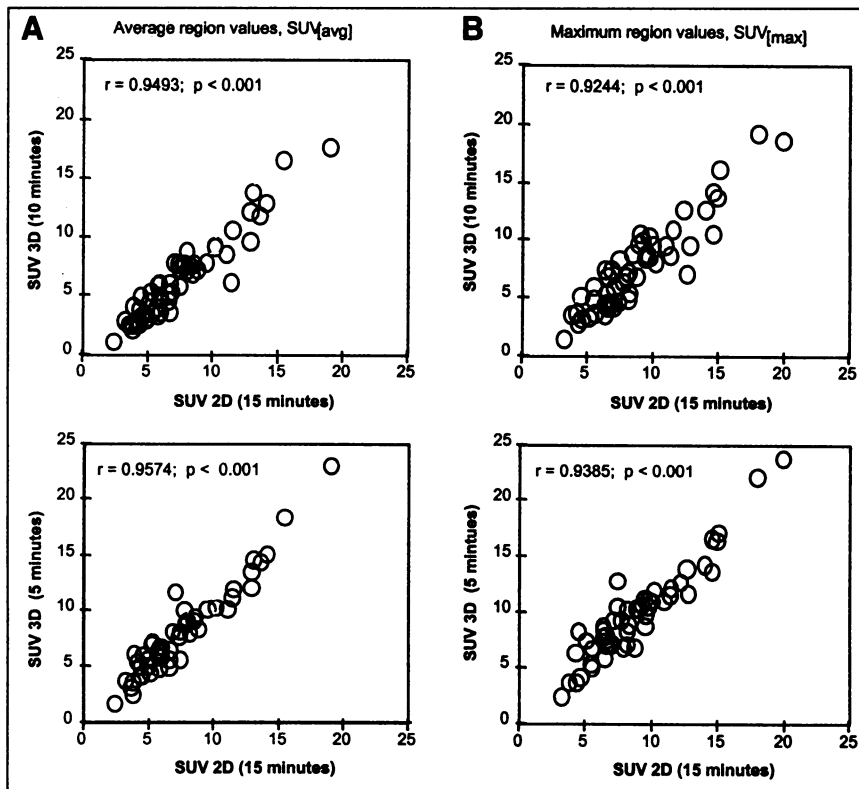


FIGURE 3. Significant positive correlation between 2-dimensional and 2 3-dimensional acquisition modes were obtained, both for $SUV_{[avg]}$ (A) and $SUV_{[max]}$ (B). Open circles represent SUVs for 53 foci studied.

Furthermore, SUVs from study₃ were not statistically correlated with time, whereas SUVs from study₁ and study₂ showed a significant positive correlation.

The intrasubject variability was higher for $SUV_{[max]}$ compared with $SUV_{[avg]}$ as indicated by the mean \pm SD percentage differences of $17\% \pm 13\%$, $19\% \pm 15\%$, and $26\% \pm 21\%$ for $SUV_{[max]2-1}$, $SUV_{[max]3-2}$, and $SUV_{[max]3-1}$; and $16\% \pm 12\%$, $17\% \pm 13\%$, and $24\% \pm 18\%$ for $SUV_{[avg]2-1}$, $SUV_{[avg]3-2}$, and $SUV_{[avg]3-1}$. Figure 4A shows, as an example, the variability between study₁ and study₃.

TABLE 3
Interdependence of Log(SUV) Values on Time Postinjection (Minutes)

Log(SUV)	<i>r</i>	<i>P</i>
Log $SUV_{[max]}$ study ₁ = $0.57 + 0.0043t_1$	0.42	0.001*
Log $SUV_{[max]}$ study ₂ = $0.65 + 0.0030t_2$	0.32	0.018*
Log $SUV_{[max]}$ study ₃ = $0.77 + 0.0020t_3$	0.22	0.11 NS
Log $SUV_{[avg]}$ study ₁ = $0.50 + 0.0042t_1$	0.38	0.005*
Log $SUV_{[avg]}$ study ₂ = $0.60 + 0.0027t_2$	0.26	0.055†
Log $SUV_{[avg]}$ study ₃ = $0.68 + 0.0021t_3$	0.20	0.14 NS

* $P < 0.05$.

† $0.05 < P < 0.1$.

t_1 = acquisition start time for all foci in study₁ (range, 40–105 min);
 t_2 = acquisition start time for all foci in study₂ (range, 51–115 min);
 t_3 = acquisition start time for all foci in study₃ (range, 70–134 min);
 NS = no statistical significance.

Patients (foci) are ordered ascending with time from the acquisition start time of the first PET study.

Data were divided into 2 independent groups, because the percentage difference of SUV between studies showed a great variability in the experimental periods up to 70 min postinjection (focus 35, Fig. 4A), and from this time point on a sharp reduction with lower variability was observed in the percentage difference between studies. In the first dataset, every pair of studies in which the first PET acquisition was started earlier than 70 min after the tracer injection was included, resulting in a mean percentage difference of $25\% \pm 17\%$ for the $SUV_{[avg]}$. This intrasubject variability was reduced to $13\% \pm 10\%$ when the second dataset was analyzed (in which the first PET study started later than 70 min after FDG injection) (Table 4). Furthermore, since the 3 PET studies were acquired consecutively, differences between studies led to differences in time. If the first PET study is started earlier than 70 min postinjection, a delay of 13 ± 2 (32 ± 3) min in the acquisition start time, i.e., difference in time between study₁ and study₂ (study₁ and study₃), will represent a mean percentage difference of 20% (31%) on SUVs, whereas when the first study is performed later than 70 min postinjection, those differences were reduced to 9% (10%). The reproducibility between the studies was also calculated, and an increase in the reliability coefficient from 0.87–0.95 was found when the first acquisition started more than 70 min after tracer injection.

In line with the analysis performed on the SUVs, the differences between the relative errors were plotted against

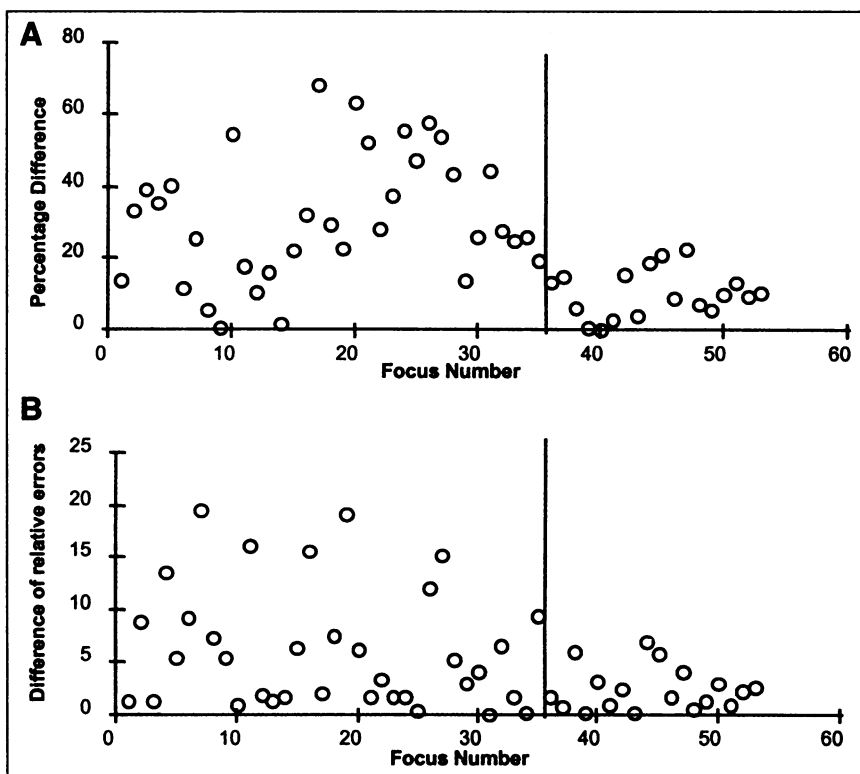


FIGURE 4. Intrasubject variability between study₁ and study₃ for SUV_[avg] values (A) and difference of relative errors of FDG distribution within ROI (B). Foci are ordered ascending with time from acquisition start time of first PET study (study₁). Vertical line, corresponding to foci 35, separates data for comparison in 2 groups: on left, first PET study started earlier than 70 min postinjection. Because 3 studies are consecutive in time, difference between study₁ and study₃ represents delay in acquisition start time of 31 ± 3 min.

the foci number ascending with time from the acquisition start time of the first PET study compared (Fig. 4B). The intrasubject variability observed on the activity distribution within each ROI was then analyzed by calculating the differences among the relative error of SUV_[avg] from the 3 studies (i.e., $(1/53)(1/3) \sum |re_{i1} - re_{i2}| + |re_{i1} - re_{i3}| + |re_{i2} - re_{i3}|$, where *re* is the relative error, *i* goes from 1–53; and 1, 2, and 3 are from PET study index). A 5% mean difference was found for the entire dataset, whereas a reduction by half, i.e., from 6.1% to 3.6% was observed when differences on relative errors were compared over the intervals 40–70 and 70–105 min postinjection. In addition, a significant inverse relationship between the uptake values (SUV_[avg]) and their relative error was observed for the 3 studies (study₁: $r = -0.53$; study₂: $r = -0.56$, and study₃: $r = -0.63$, with $P < 0.001$), yielding a stronger negative correlation with data from study₃.

TABLE 4
Mean Percentage Difference, SD, and Reliability Coefficient of the SUVs_[avg] from 3 Studies

Acquisition time postinjection (first PET study)	Mean percentage difference	95% CV	Reliability coefficient
40–134 min	19% ± 15%	17–21	0.90
40–70 min	25% ± 17%	21–28	0.87
70–134 min	13% ± 10%	11–16	0.95

CV = coefficient of variation.

The mean ± SD of different SUV normalizations, both for SUV_[max] and SUV_[avg], are shown in Table 5. No dependency was found for SUV and its different normalizations, with TBW, LBM, BSA, or PGL. On the basis of the fact that normalization methods might be more helpful in patients who are significantly under- or overweight, the normalization was tested in a subset of such patients, yielding 9 foci for the study (3,11,13,19). In this group, only a negative correlation was found between PGL and SUV ($r = -0.52$, $P = 0.038$), SUV_{LBM} ($r = -0.53$, $P = 0.033$), and SUV_{BSA}

TABLE 5
Different Normalized SUV of FDG Uptake in Lung Foci

Parameter	Study ₁	Study ₂	Study ₃
Maximum SUVs			
SUV	8.1 ± 3.8	8.6 ± 3.6	10.2 ± 4.2
SUV _(LBM)	6.9 ± 3.3	7.3 ± 3.0	8.6 ± 3.5
SUV _(BSA)	8.5 ± 4.0	9.0 ± 3.7	10.6 ± 4.2
SUV _(PGL)	7.6 ± 3.9	8.0 ± 3.5	9.5 ± 4.1
SUV _(PGL-LBM)	6.4 ± 3.1	6.7 ± 2.8	8.0 ± 3.4
SUV _(PGL-BSA)	7.2 ± 3.4	7.6 ± 3.1	9.0 ± 3.6
Average SUVs			
SUV	6.8 ± 3.6	7.3 ± 3.4	8.5 ± 4.0
SUV _(LBM)	5.8 ± 3.1	6.2 ± 2.9	7.2 ± 3.4
SUV _(BSA)	7.2 ± 3.7	7.6 ± 3.5	8.8 ± 4.1
SUV _(PGL)	6.4 ± 3.5	6.8 ± 3.2	7.9 ± 3.9
SUV _(PGL-LBM)	5.4 ± 2.9	5.7 ± 2.6	6.7 ± 3.2
SUV _(PGL-BSA)	6.1 ± 3.1	6.5 ± 3.0	7.5 ± 3.5

Values are mean ± SD.

($r = -0.54$, $P = 0.031$). On the other hand, when normalization of these values to PGL was applied, no significant correlation was observed for SUV_{PGL} , $SUV_{PGL-LBM}$, and $SUV_{PGL-BSA}$.

DISCUSSION

Despite the multiple advantages of 3-dimensional over 2-dimensional PET and its wide use for brain imaging, the number of centers actively engaged in performing 3-dimensional PET body studies is still comparatively limited. Some of the problems involved in its use in clinical practice have been addressed elsewhere (33).

The large scatter component present in 3-dimensional PET quantitative analysis makes both attenuation and scatter correction essential. The generally accepted 2-dimensional PET measurements are usually accurate to within 5% of the true value. Townsend et al. (5) have shown that 3-dimensional PET with scatter and attenuation correction is as accurate as 2-dimensional PET with reported agreement to within better than 5%, whereas Dhawan et al. (4) reported maximum differences of 14.7% in the measurement of regional glucose metabolism.

In addition, the issues involved in practical 3-dimensional PET imaging of the torso have not been studied in so much detail as in brain imaging. Badawi et al. (2) investigated under which conditions the 3-dimensional mode offers an improvement over the 2-dimensional mode for different torso phantoms and found that the scatter may rise to well above 50% of total signal when scanning the phantom of an obese adult's chest. These factors, as well as the movement of the thoracic cavity and the presence of the heart, prompt us to query the accuracy of 3-dimensional quantitative analysis of the torso.

3-Dimensional Versus 2-Dimensional Semiquantitative Analysis

We have evaluated the nonkinetic analysis in a group of 21 patients with nodular lung lesions using the time after injection and the scan time as parameters. Our results showed a strong correlation between SUVs obtained from the 2-dimensional mode (study₂: conventional 15-min scan) and both 3-dimensional acquisitions (study₁: 10-min scan, study₃: 5-min scan) (Fig. 3). The mean percentage differences between both acquisition modes, i.e., between study₁ and study₂ and study₂ and study₃, were about 17%. These differences could be explained by considering the time that elapses between dose injection and PET scanning. It has been shown that SUV will differ, depending on the time when emission data are acquired (28). In this study, there was a mean difference in the acquisition start time of 13 ± 2 min (study₁ and study₂) and 18 ± 2 min (study₃ and study₂). If all studies had been performed at exactly the same time after injection, the mean percentage difference should probably have been reduced. Nevertheless, when this factor is considered and addressed as a covariant in ANOVA, no statistically significant difference between uptake values

from both 2-dimensional and 3-dimensional acquisition mode was found.

The most important consequence of these results is that 2-dimensional and 3-dimensional PET are equally suitable for clinical nonkinetic analysis, and that 3-dimensional semiquantitative PET is a realistic alternative to the conventional 2-dimensional acquisition mode. Such an alternative would lead to a decrease in the scanning time from 10–20 (2-dimensional, Table 1) to 5 min (3-dimensional), achieving similar results and reducing exploration time and patient discomfort.

Because 2-dimensional and 3-dimensional acquisition modes are interchangeable, our experimental three-step protocol may be considered a dynamic acquisition with 3 frames of 10, 15, and 5 min, respectively. Hence, our aim was to determine which frame could be used to optimize the scanning parameters and improve the employment of the SUV on the routine clinical application.

To date, the SUV is the most commonly used index to determine the malignancy/benignancy of lesions in clinical routine (19,20). Nonetheless many sources of variability must be controlled to avoid oversimplifying the inherently complicated metabolic processes (34).

Time Postinjection

The commonly adopted SUV formalism is confined to the measurement of radioactivity concentration at a fixed time point, leading to criticism of what would be the most appropriate time for assessment of tumor metabolism. As can be observed in Table 1, the main reported lung studies have performed the semiquantitative analysis at very different postinjection time points. Hamberg et al. (35) have shown that the FDG uptake in lung carcinoma does not plateau for several hours. Lowe et al. (36) proposed an optimum protocol for imaging pulmonary abnormalities at approximately 50 min after injection, and Keyes et al. (34) observed that SUV in lung tumor increases as much as 40% between 30 and 60 min postinjection. Our results support those findings, showing that when 2 PET scans are performed on the same patient and the first is done earlier than 70 min after FDG injection, SUVs derived from both acquisitions show a great variability. This estimation is obtained by extracting from the 3 PET studies the mean percentage difference. Hence, a delay in the acquisition start time of 13 min implies a difference of 20% in SUVs; that is increased to 31% when the second study is started 32 min later in time. These SUV differences are considerably reduced and become quite stable (i.e., difference of 9% and 10%, respectively) by increasing the delay between the administration of FDG and the start of the PET acquisition up to at least 70 min. In addition, when the dependency of SUV values from each study on the corresponding acquisition start time was calculated, no correlation between data derived from study₃ and the acquisition start time (ranging from 70–134 min after injection) was observed, whereas a positive correlation for study₁ and study₂ with time postinjection was found. In this case, the delay between tracer

administration and PET scanning ranged from 40–105 and 51–115 min, respectively.

Thus, when there is a need to compare the SUV values obtained from different patients, or those obtained from the same patient, as in the studies where the effect of treatment is analyzed, it is recommended that the acquisition of the emission data begin more than 70 min after injection. This would minimize error resulting from great variability at early stages, thus improving the use of the SUV.

Relative Error of $SUV_{[avg]}$

The relative error of $SUV_{[avg]}$ was calculated to estimate the combined effect of intrinsic tumor heterogeneity and ROI count statistics. Functional heterogeneity, as well as a mixture of different cell populations and necrotic tissue, is always present in the tumoral tissue. Because of the limited spatial resolution of the PET scanners, the presence of a heterogeneous distribution of FDG concentration within the ROI must be considered, especially when quantitative measurements are required. The influence of tissue heterogeneity on FDG quantification has been previously investigated by others (37,38).

In this study, the negative correlations obtained from the 3 PET studies between the SUVs and their relative errors indicate that regions with high FDG metabolic uptake display a less heterogeneous distribution of tracer accumulation. Our results also indicate that when 2 PET studies are performed on the same tumor, the differences observed in the relative error of the SUVs values could be circumvented if the PET studies are performed at least 70 min after tracer injection.

From the present data, an acquisition beginning at least 70 min after tracer injection seems to provide less variation on the SUV's relative error. However, to analyze the influence on the relative error from the tissue's intrinsic heterogeneity and the ROI count statistics, further investigation and appropriate mathematical models are required.

ROI Placing and Size

The last methodological consideration to be addressed in this study was the size and placement of the ROIs. Kuwert et al. (39) found that increasing the ROI width from 2 to 20 mm led to a significant decrease in caudate regional cerebral metabolic rate of glucose ($rCMR_{glc}$) by about 66%, and suggested the maximum value as the best way to discriminate between groups of subjects believed to differ with respect to $rCMR_{glc}$. Keyes et al. (34) showed that when the average SUVs were used, the distortion introduced could be significant. Our results showed that, although the maximum SUV values are about 19% greater than the averages values, the differences between studies are lower if the average values are used. Indeed, when the peak values— $SUV_{[max]}$ —were used, a borderline significant difference between the 3 studies was found, whereas a clearly nonsignificant difference was observed using the averaged ones, $SUV_{[avg]}$. This could be attributed to a reduction in the influence of statistical image noise when more than 1 pixel is included in

the ROI. These results are in concordance with those reported by Avril et al. (40), who found that the use of maximum activity values resulted in a significantly lower diagnostic accuracy than the use of average activity values.

Normalization

Other possible sources of variability are derived from inherently different characteristics of each patient, such as TBW, LBM, BSA, and PGL. Zasadny et al. (24) have described a positive correlation between SUV and body weight for liver, blood, and spleen, and no correlation for marrow and normal breast. Kim et al. (25) showed similar results: the dependency of SUV_{LBM} and SUV_{BSA} on TBW, and moderate dependency of SUV_{LBM} on height, LBM, and BSA. They proposed SUV_{BSA} as the best normalization, because no dependency was shown on TBW or body size. We have found no correlation between different SUV normalization values and LBM, BSA, TBW, and height, either when all patients are considered in a single set, or when only a reduced set of over- or underweight patients is considered. These discrepancies could be explained by the fact that in the referred works (24,25), the ROIs were placed in normal tissue, studying the influence of the individual characteristics on the normal tissue, whereas our analysis was performed by placing the 2 ROIs on the plane and over the pixels of highest intensity for each foci. Hence, we studied the influence of LBM, BSA, TBW, and height on lung tumor foci, as in the clinical situation, in which characterization of abnormal foci is desirable. Our results show that no differences or advantages can be found using any of the proposed normalizations of SUV. Similar results were found by Avril et al. (40), showing that no differences between SUV and its different normalizations were obtained to differentiate benign from malignant breast tissue.

It is widely known that PGL at the time of the study also has a major effect on the SUV. Langen et al. (27) investigated 15 patients with lung cancer and reported a marked decrease in FDG after infusing sufficient glucose to approximately double the fasting conditions. Lindholm et al. (28) also found similar results in a group of patients with head and neck cancer and in rats with breast cancer. The first correlation among SUV and its different normalization with PGL for all patients showed no significant correlation; this can be explained because the majority of the patients had "normal" PGL. On the other hand, when a selection of patients was analyzed, a strong dependency was found, dependency that was eliminated when the SUV values were corrected by the PGLs. The use of glucose normalization in those cases can also compensate for the slight increase (<4% of the coefficients of variation of the SUV_{PGL}) over the other normalizations, with less variability.

In summary, our results suggest that the 4 following practical strategies should be applied to optimize the use of standard uptake value:

1. Start the acquisition of the emission data at the same time postinjection (≥ 70 min).

2. Use a small ROI, rather than 1-pixel ROI, to improve counting statistics, while minimizing noise.
3. Place such an ROI over the highest-activity pixels to obtain a lower relative error for the tracer uptake.
4. Correct the SUV values by the PGLs to take account of the decrease of FDG uptake that may be observed in patients with hyperglycemia.

CONCLUSION

To evaluate the potential of 3-dimensional PET imaging in clinical practice, the current study was designed to investigate the accuracy of 3-dimensional semiquantitative PET in patients with nodular lung lesions. Although further investigations to evaluate the influence of increased scatter and random and dead time on the image quality are needed, the present results suggest that 2-dimensional and 3-dimensional acquisitions are equally suitable for clinical nonkinetic studies.

We have shown that the effect of inaccuracies on the calculation of SUV can be minimized by increasing the time elapsed between the administration of FDG and the time of scanning up to at least 70 min. Furthermore, combination of a short, 5-min 3-dimensional acquisition at least 70 min after tracer injection with the positioning of a small ROI on the plane and over the pixels of highest activity can be used to minimize 3 important sources of error in semiquantitative PET: (1) the variability in the calculation of SUV that results from the heterogeneous distribution of FDG within the tumoral tissue, (2) the statistical noise, and (3) the variation of SUVs over time. On the other hand, no advantages were observed when SUVs were corrected either by LBM or BSA. Conversely, we have found that SUV is influenced by PGL in pulmonary lesions for patients who are significantly under- or overweight, thus suggesting the possibility of considering the normalization of SUV by PGL as the best semiquantitative value for 3-dimensional PET of the torso.

It is clear that when the time that elapses between the tracer administration and the beginning of the emission studies is prolonged, the counting rate will be diminished. In this situation the use of 3-dimensional acquisition mode could compensate for this effect at longer postinjection periods. Furthermore, we have shown that the SUVs obtained from the 3-dimensional studies performed after the referred 70 min do not vary appreciably with time.

We can finally conclude that the use of 3-dimensional PET semiquantitative studies is not only feasible in thoracic tumors but also worthwhile, because the reduction in PET scanner occupancy time permits us to improve the overall patient care and makes for better scheduling of studies. Our work encourages further investigation of 3-dimensional imaging in other clinical applications.

ACKNOWLEDGMENTS

We thank the staff of the Cyclotron Unit for radioisotope and tracer production. The authors also acknowledged the

nuclear medicine technologist support in acquiring the imaging and R. Breeze for revising the English text. R. Calvo is supported by a Siemens fellowship.

REFERENCES

1. Cherry SR, Dahlbom M, Hoffman EJ. 3D PET using a conventional multislice tomograph without septa. *J Comput Assist Tomogr*. 1991;15:655-668.
2. Badawi RD, Marsden PK, Cronin BF, Sutcliffe JL, Maisey MN. Optimization of noise-equivalent count rates in 3D PET. *Phys Med Biol*. 1996;41:1755-1776.
3. Zasadny KR, Kison PV, Wahl RL. Practical tumor activity quantification strategies in 2D and 3D PET [abstract]. *J Nucl Med*. 1998;39:258P.
4. Dhawan V, Kazumata K, Roberson W, et al. Quantitative brain PET: comparison of 2D and 3D acquisition [abstract]. *J Nucl Med*. 1997;38:195P.
5. Townsend DW, Price JC, Mintun MA, et al. Scatter correction for brain receptor quantitation in 3D PET. In: Myers R, Cunningham VJ, Bailey DL, Jones T, eds. *Quantification of Brain Function Using PET*. San Diego, CA: Academic Press;1996:76-81.
6. Kinahan PE, Jadhali F, Sashin D, et al. A comparison of 2D and 3D abdominal PET imaging [abstract]. *J Nucl Med*. 1995;36:7P.
7. Marsden PK, Badawi RD, Wong JCH, Maisey MN. Validation of 3D positron emission tomography (PET) for cardiac scanning in young children. *Nucl Med Commun*. 1996;17:283.
8. Kubota K, Matsuzawa T, Fujiwara T, et al. Differential diagnosis of lung tumor with positron emission tomography: a prospective study. *J Nucl Med*. 1990;31:1927-1933.
9. Gupta NC, Frank AR, Naresh AD, et al. Solitary pulmonary nodules: detection of malignancy with PET with 2-[F-18]-fluoro-2-deoxy-D-glucose. *Radiology*. 1992;184:441-444.
10. Patz EF, Lowe VJ, Hoffman JM, et al. Focal pulmonary abnormalities: evaluation with F-18 fluorodeoxyglucose PET scanning. *Radiology*. 1993;188:487-490.
11. Lowe VJ, Hoffman JM, DeLong DM, Patz EF, Coleman RE. Semiquantitative and visual analysis of FDG-PET images in pulmonary abnormalities. *J Nucl Med*. 1994;35:1771-1776.
12. Hübner, KF, Buonocore E, Gould H, et al. Differentiating benign from malignant lung lesions using "quantitative" parameters of FDG PET images. *Clin Nucl Med*. 1996;21:941-949.
13. Regé SD, Hoh CK, Glaspy JA, et al. Imaging of pulmonary mass lesions with whole-body positron emission tomography and fluorodeoxyglucose. *Cancer*. 1993;72:82-90.
14. Wahl RL, Quint LE, Greenough RL, Meyer CR, White RI, Orringer MB. Staging of mediastinal non-small cell lung cancer with FDG PET, CT, and fusion images: preliminary prospective evaluation. *Radiology*. 1994;191:371-377.
15. Duhaylongsod FG, Lowe VJ, Patz EF, Vaughn AL, Coleman RE, Wolfe WG. Detection of primary and recurrent lung cancer by means of F-18 fluorodeoxyglucose positron emission tomography (FDG PET). *J Thorac Cardiovasc Surg*. 1995;110:130-140.
16. Bury TH, Paulus P, Dowlati A, et al. Staging of the mediastinum: value of positron emission tomography imaging in non-small cell lung cancer. *Eur Respir J*. 1996;9:2560-2564.
17. Steinert HC, Hauser M, Allemann F, et al. Non-small cell lung cancer: nodal staging with FDG PET versus CT with correlative lymph node mapping and sampling. *Radiology*. 1997;202:441-446.
18. Higashi K, Nishikawa T, Seki H, et al. Comparison of fluorine-18-FDG PET and thallium-201 SPECT in evaluation of lung cancer. *J Nucl Med*. 1998;39:9-15.
19. Rigo P, Paulus P, Kaschten R, et al. Oncological applications of positron emission tomography with fluorine-18 fluorodeoxyglucose. *Eur J Nucl Med*. 1996;23:1641-1674.
20. Strauss LG, Conti PS. The application of PET in clinical oncology. *J Nucl Med*. 1991;32:623-648.
21. Di Chiro G, Brooks AR. PET quantitation: blessing and curse [editorial]. *J Nucl Med*. 1988;29:1603-1604.
22. Hawkins RA, Choi Y, Huang S, Messa C, Hoh CK, Phelps ME. Quantitating tumor glucose metabolism with FDG and PET [editorial]. *J Nucl Med*. 1992;33:339-344.
23. Fischman AJ, Alpert NM. FDG-PET in oncology: there's more to it than looking at pictures. *J Nucl Med*. 1993;34:6-11.
24. Zasadny KR, Wahl RL. Standardized uptake values of normal tissues at PET with FDG: variation with body weight and a method for correction. *Radiology*. 1993;189:847-850.
25. Kim CK, Gupta NC, Chandramouli B, Alavi A. Standardized uptake values of

- FDG: body surface area correction is preferable to body weight correction. *J Nucl Med.* 1994;35:164-167.
26. Schomburg A, Bender H, Reichel C, et al. Standardized uptake values of fluorine-18 fluorodeoxyglucose: the value of different normalization procedures. *Eur J Nucl Med.* 1996;23:571-574.
 27. Langen K-J, Braun U, Kops ER, et al. The influence of plasma glucose levels on fluorine-18-fluorodeoxyglucose uptake in bronchial carcinomas. *J Nucl Med.* 1993;34:355-359.
 28. Lindholm P, Minn H, Leskinen-Kallio S, Bergman J, Ruotsalainen U, Joensuu H. Influence of the blood glucose concentration on FDG uptake in cancer—a PET study. *J Nucl Med.* 1993;34:1-6.
 29. Brix G, Zaers J, Adam L-E, et al. Performance evaluation of a whole-body PET scanner using the NEMA protocol. *J Nucl Med.* 1997;38:1614-1623.
 30. Bland JM, Altman DG. Transforming data. *Br Med J.* 1996;312:770.
 31. Vingerhoets FJG, Snow BJ, Schulzer M, et al. Reproducibility of fluorine-18-6-fluorodopa positron emission tomography in normal human subjects. *J Nucl Med.* 1994;35:18-24.
 32. Minn H, Zasadny KR, Quint LE, Wahl RL. Lung cancer: reproducibility of quantitative measurements for evaluating 2-[F-18]-fluoro-2-deoxy-D-glucose uptake at PET. *Radiology.* 1995;196:167-173.
 33. Badawi RD. 3-D mode acquisition in clinical PET [editorial]. *Nucl Med Commun.* 1997;18:801-804.
 34. Keyes JWJ. SUV: standard uptake or silly useless values? *J Nucl Med.* 1995;36:1836-1839.
 35. Hamberg LM, Hunter GJ, Alpert NM, Choi NC, Babich JW, Fischman AI. The dose uptake ratio as an index of glucose metabolism: useful parameter or oversimplification? *J Nucl Med.* 1994;35:1308-1312.
 36. Lowe VJ, DeLong M, Hoffman JM, Coleman RE. Optimum scanning protocol for FDG-PET evaluation of pulmonary malignancy. *J Nucl Med.* 1995;36:883-887.
 37. Lucignanni G, Schmidt KC, Moresco RM, et al. Measurement of regional cerebral glucose utilization with fluorine-18-FDG and PET in heterogeneous tissues: theoretical considerations and practical procedure. *J Nucl Med.* 1993;34:360-369.
 38. Wu H-M, Huang S-C, Choi Y, Hoh CK, Hawkins RA. A modeling method to improve quantitation of fluorodeoxyglucose uptake in heterogeneous tumor tissue. *J Nucl Med.* 1995;36:297-306.
 39. Kuwert T, Ganslandt T, Jansen P, et al. Influence of size of region of interest on PET evaluation of caudate glucose consumption. *J Comput Assist Tomogr.* 1992;16:789-794.
 40. Avril N, Bense S, Ziegler SI, et al. Breast imaging with fluorine-18-FDG PET: quantitative image analysis. *J Nucl Med.* 1997;38:1186-1191.